JOURNAL OF SOLID STATE CHEMISTRY 2, 167–175 (1970)

Pentavalent Ion Substitutions in the Apatite Structure Part B. Color*

D. A. GRISAFE† AND F. A. HUMMEL‡

College of Earth and Mineral Sciences, The Pennsylvania State University, University Park, Pennsylvania 16802

Received October 24, 1969

Pentavalent chromium or manganese substituted into the pentavalent ion site always produced green and blue to green apatites, respectively. The positions of the absorption bands of the CrO_4^{3-} or MnO_4^{3-} oxyanions were not appreciably affected by changes in the composition of the apatite. Possible models based on the Ballhausen–Liehr molecular orbital scheme were used to interpret the reflectance spectra of apatites containing pentavalent vanadium, chromium, and manganese.

Introduction

Very little information is available for apatites containing pentavalent coloring ions. In the present work, reflectance spectra are presented for various alkaline earth fluor- and chlorapatites containing pentavalent vanadium, chromium and manganese. A brief comparison or available molecular orbital schemes for tetrahedral oxyanions shows that the model of Ballhausen and Liehr (*1*) can be used to identify the transitions that give rise to the absorption bands in the reflectance spectra of these apatites.

Literature

In discussing pentavalent ion color centers in the tetrahedrally coordinated sites of apatite, it must be emphasized that these oxyanions are considerably covalent in nature. Thus, crystal field theory is not as valid for interpreting the absorption spectra of these ions as molecular orbital theory.

Analogies with solution spectra for these tetrahedrally coordinated color centers are invaluable. Carrington and Symons (*2*) presented the ultraviolet and visible absorption spectra of the MnO_4^{3-} and MnO_4^{2-} and MnO_4^{-} ions in aqueous solutions. Bailey and Symons (*3*) presented similar absorption curves for the CrO_4^{3-}, CrO_4^{2-}, and Cr^{3+} ions in aqueous solutions. Carrington et al. (*4*) summarized the spectra of the chromium and manganese oxyanions and made tentative identifications of the electronic transitions using the molecular orbital designation derived by Wolfsberg and Helmholz (*5*) for the CrO_4^{2-} ion. Carrington and Symons (*6*) later applied the molecular orbital model of Ballhausen and Liehr (*1*) to the spectra of these ions. The results using the two molecular orbital models are given in Table I.

Results and Discussion

Vanadium

Pentavalent vanadium is not considered to be a coloring ion. However, it can exert a modifying influence on the color of apatites.

Pentavalent vanadium has no d electrons and by crystal field theory should have no absorption bands. However, it is well-known that vanadates absorb in the ultraviolet region. Such behavior can be explained by a charge transfer mechanism made possible by molecular orbital theory.

As expected, the vanadate apatites showed no absorption maxima in the visible region. They did show some absorption in the blue region stemming from the tail of the ultraviolet absorption. The lead apatite showed the strongest absorption in the blue region which accounted for its pale yellow color.

* Contribution No. 69-8 from the College of Earth and Mineral Sciences, the Pennsylvania State University, University Park, Pa.

† D. A. Grisafe is currently employed by Sylvania Electric Products, Inc. Chemical and Metallurgical Division, Towanda, Pa.

‡ F. A. Hummel is Professor of Ceramic Science, Materials Science Department, the College of Earth and Mineral Sciences, The Pennsylvania State University, University Park, Pa.

TABLE I

ELECTRONIC TRANSITIONS AND ABSORPTION MAXIMA WAVELENGTHS (mμ) OCCURRING IN TETRAHEDRAL OXYANIONS OF CHROMIUM AND MANGANESE IN AQUEOUS SOLUTION

Electronic Transition	CrO_4^{2-}	CrO_4^{3-}	MnO_4^-	MnO_4^{2-}	MnO_4^{3-}
		Carrington, Schonland, and Symons (*4*)			
$3t_2 \rightarrow 2a_1$	—	625	—	605	675
$t_1 \rightarrow 3t_2$	373	355	546	436	328
$3t_2 \rightarrow 2e$	—	—	—	351	325
$2t_2 \rightarrow 3t_2$	273	—	310	299	216
		Carrington and Symons (*6*)			
$t_1 \rightarrow e$	373($^1T_2$)	No data given	546($^1T_2$)	605($^2T_1$) 436($^2T_2$)	675($^3T_1$)
$t_1 \rightarrow t_2$	273($^1T_2$)	—	310($^1T_2$)	351($^2T_1$) 299($^2T_2$)	325($^3T_1$)
$e \rightarrow t_2$	—	—	—	833($^2T_2$)	—

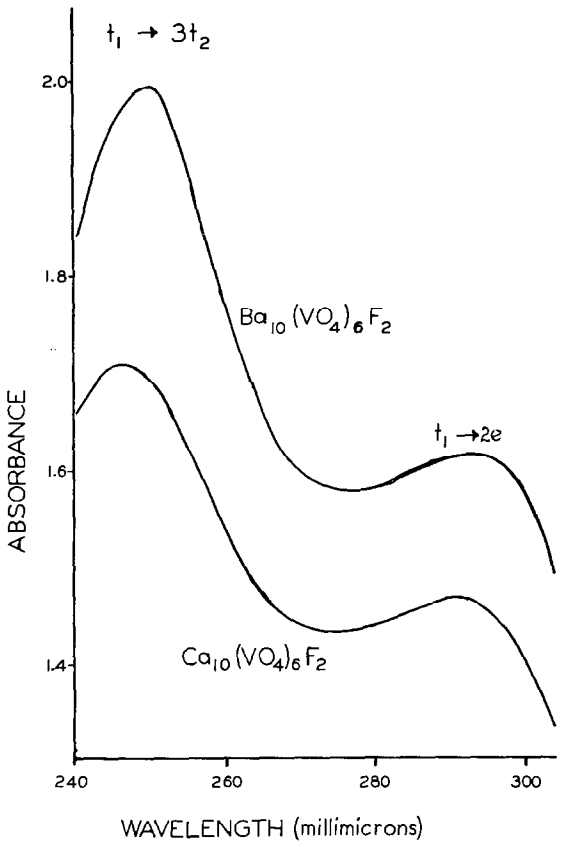

FIG. 1. Ultraviolet reflectance spectra for $Ca_{10}(VO_4)_6F_2$ and $Ba_{10}(VO_4)_6F_2$.

Typical ultraviolet reflectance spectra for calcium and barium fluorvanadate apatites are shown in Fig. 1. Despite the large difference in size between the calcium and barium ions and the distorted nature of the calcium apatite, the spectra are very similar.

Wolfsberg and Helmholz (*5*) calculated the molecular orbital energies for the MnO_4^- and CrO_4^{2-} oxyanions. Both of these XO_4 ions have a central atom with no d electrons and are isoelectronic with the VO_4^{3-} ions. According to their designation, the two highest energy orbitals of the ground state of these ions were $(2t_2)^6$ and $(t_1)^6$ and the two observed absorption bands for MnO_4^- and CrO_4^{2-} originated from electronic transitions to the next available level, $3t_2$, specifically the $t_1 \rightarrow 3t_2$ and $2t_2 \rightarrow 3t_2$ transitions. Carrington et al. (*4*) examined the MnO_4^- and CrO_4^{2-} ions and also observed two absorption bands as noted in Table I. They plotted the ionic radius of the central metal atom of several oxyanions isoelectronic with MnO_4^- versus the first absorption maximum. The resulting plot was a straight line which showed that the first transition for VO_4^{3-} occurred around 270 mμ. Using the same procedure for the second transition suggests that the latter transition in VO_4^{3-} (not observed by the above authors) should occur at a slightly lower wavelength than the first transition. Hence, the absorption bands around 290 and 250 mμ in the VO_4^{3-} spectra in Fig. 1 fit into the above scheme and on the basis of the Wolfsberg–Helmholz model, can be assigned to electron jumps between the $t_1 \rightarrow 3t_2$ and $2t_2 \rightarrow 3t_2$ levels, respectively.

Ballhausen and Liehr (*1*) derived a different model to explain the spectra of the MnO_4^- and CrO_4^{2-} oxyanions in which a doubly degenerate *e* level was located between the t_1 and $3t_2$ levels. This model was verified by the electron spin resonance measurements of Carrington et al. (*7*) for pentavalent manganese. To interpret the reflectance spectra of vanadium by the Ballhausen–Liehr model requires the energy of the *e* level (2*e*) to be much closer to the $3t_2$ level than the t_1. The transitions at 290 and 250 mμ for VO_4^{3-} would be between the $(t_1)^6$ ground state to the excited configurations $(t_1)^5(2e)$ and $(t_1)^5(3t_2)$, respectively. Both of these absorptions are designated as $^1A_1 \rightarrow {}^1T_2$ transitions.

The Ballhausen–Liehr model was also used by Dijkgraaf (*8*) to explain the two ultraviolet absorption peaks of $TiCl_4$. The latter author used a different model to explain the ultraviolet absorption of V^{5+} in the highly distorted tetrahedral $VOCl_3$ molecule. Due to the distortion, the triply degenerate levels were split into *e* and *a* levels so the ground state configuration $(t_1)^6$ was split into $(4e)^4$ $(1a_2)^2$. The ultraviolet absorption bands by this model were represented as transitions from the $(1a_2)^2$ to the $(1a_2)(5e)$ and $(1a_2)(6e)$ configurations, respectively. It must be emphasized that the 5*e* level corresponds to the Ballhausen–Liehr 2*e* orbital and that the 6*e* level originates from the splitting of the $3t_2$ level of the Ballhausen–Liehr model. The above models are represented schematically in Fig. 2.

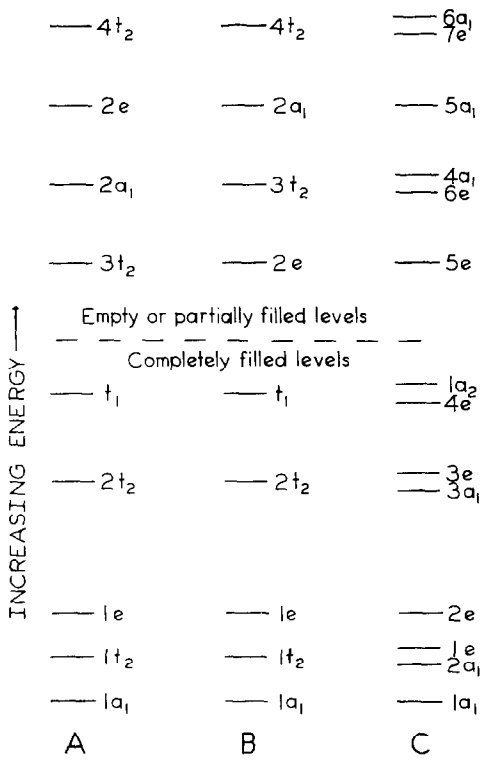

FIG. 2. Schematic representation of molecular orbital models for tetrahedrally oriented d^0 cations derived by
A = Wolfsberg and Helmholz (*5*) for MnO_4^- and CrO_4^{2-};
B = Ballhausen and Liehr (*1*) for MnO_4^- and CrO_4^{2-};
C = Dijkgraff (*8*) for $VOCl_3$.

The Dijkgraaf model is probably the most accurate model for interpreting the spectra of ions in a highly distorted tetrahedral environment. However, the splitting of the t levels should be less in the apatite structure compared to the $VOCl_3$ molecule so the more simple Ballhausen–Liehr model is sufficient to explain the reflectance spectra of the VO_4^{3-} ion in the apatite structure. The latter model will be used in the following sections to interpret the spectra of pentavalent chromium and manganese in the apatite structure.

Chromium

Pentavalent chromium possesses a d^1 electronic configuration. By crystal field theory, the ground state of the free ion would be ^2D which in the presence of a tetrahedral crystal field would split into the ^2E and $^2T_2$ states. One would normally expect to see a single absorption band such as that observed for Ti^{3+} [McClure (*9*)].

The visible reflectance spectra of apatites containing pentavalent chromium always showed two or more absorption bands (extreme blue and extreme red). Two absorption bands (extreme blue and red) were reported for the CrO_4^{3-} ion in aqueous solution by Bailey and Symons (*3*). Therefore, a molecular orbital model is necessary to explain the spectra of the CrO_4^{3-} oxyanion.

The reflectance spectra of the apatites containing Cr^{5+} are very similar but somewhat different from the solution spectrum of Bailey and Symons (*3*). The former spectra are always characterized by a relatively broad band occurring in the extreme red and a stronger band peaking between 350 and 370 mμ. Typical spectra are shown in Fig. 3. The above solution spectrum exhibits bands at 625 and 355 mμ.

Figure 3 shows the reflectance spectra of the alkaline earth fluorapatites containing 20 mole % chromium substituted for phosphorus or vanadium. All of the samples were green. It is important to note that for a given pentavalent host ion the spectra are very similar which implies that in apatite the positions of the CrO_4^{3-} ion absorptions are relatively independent of the alkaline earth ion. The latter observation was found to be true at all concentra-

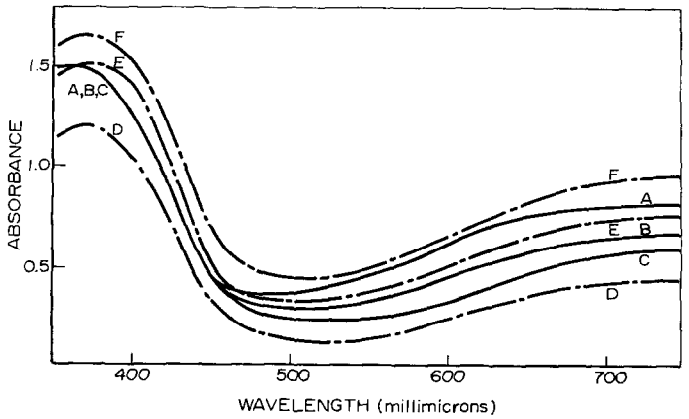

FIG. 3. Reflectance spectra of alkaline-earth fluorphosphate apatites containing 20 mole % pentavalent chromium for phosphorus or vanadium.

$A = Ca_{10}(PO_4)_{4.8}(CrO_4)_{1.2}F_2$;
$B = Sr_{10}(PO_4)_{4.8}(CrO_4)_{1.2}F_2$;
$C = Ba_{10}(PO_4)_{4.8}(CrO_4)_{1.2}F_2$;
$D = Ca_{10}(VO_4)_{4.8}(CrO_4)_{1.2}F_2$;
$E = Sr_{10}(VO_4)_{4.8}(CrO_4)_{1.2}F_2$;
$F = Ba_{10}(VO_4)_{4.8}(CrO_4)_{1.2}F_2$.

tions of chromium. The reflectance spectra of the phosphate-chromate and vanadate-chromate apatites are also similar. The absorption maximum of the near ultraviolet band is slightly affected by the pentavalent ion. The maximum occurs at higher wavelengths in the vanadate host lattice. With increasing concentration of chromium, no change was observed in the maximum position for the phosphate-chromate series but in the vanadate chromate series, the band position shifted from 370 $m\mu$ (5 mole % Cr^{5+}) to around 350 $m\mu$ (100 mole % Cr^{5+}).

Using the Ballhausen–Liehr molecular orbital model, the location of the 2*e* orbital between the t_1

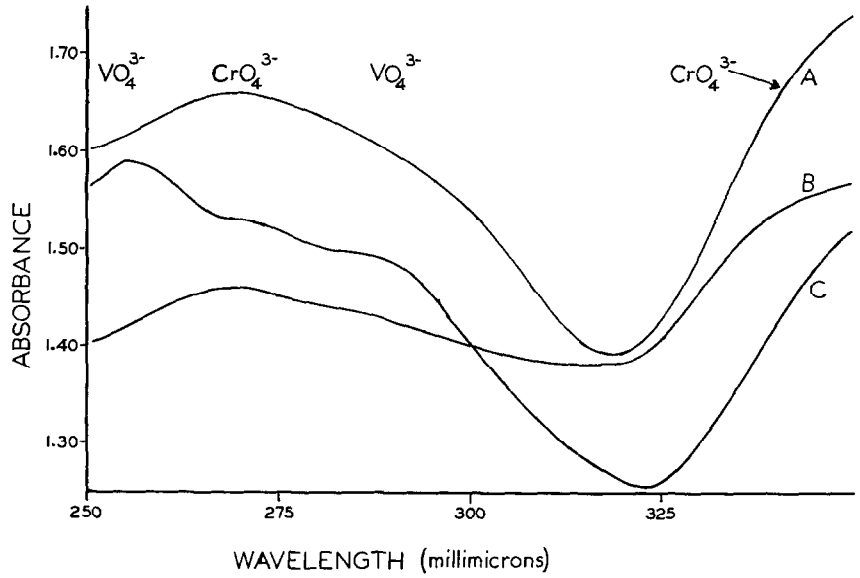

FIG. 4. Ultraviolet reflectance spectra of apatites containing pentavalent chromium.

$A = Ca_{10}(PO_4)_{4.8}(CrO_4)_{1.2}F_2$;
$B = Sr_{10}(CrO_4)_6F_2$;
$C = Ba_{10}(VO_4)_{4.8}(CrO_4)_{1.2}F_2$.

and $3t_2$ orbitals allows configurational transitions from the $(t_1)^6(2e)^1$ ground state ($=^2E$) involving $t_1 \rightarrow 2e$, $2e \rightarrow 3t_2$ and $t_1 \rightarrow 3t_2$ electron jumps. In tetrahedral symmetry, each of these transitions allows both T_1 and T_2 excited states. The following discussion represents a possible model to explain the origin of absorptions due to Cr^{5+}, but it must be emphasized that there is no unique solution to such an assignment.

In the ultraviolet region a band at 270 mμ (not previously reported) was observed in the alkaline earth chromate apatites and the vanadate–chromate solid solutions. This band is not always resolved in the vanadate–chromate apatites since the ultraviolet absorption bands of the VO_4^{3-} ion (250 and 290 mμ) tend to mask the CrO_4^{3-} band. Only when the vanadium is replaced by 50 mole % or more chromium does the 270-mμ band become easily detectable. Representative spectra showing this band are illustrated in Fig. 4. The position of the band is little affected by the composition of the apatite.

It is possible that the 270-mμ band arises from the $t_1 \rightarrow 3t_2$ electron jump. As pointed out in the discussion of the MnO_4^{2-} spectrum by Carrington and Symons (*6*) the $t_1 \rightarrow 3t_2$ $\{(t_1)^6(2e)^1 \rightarrow (t_1)^5(2e)^1(3t_2)^1\}$ transition gives rise to both $^2T_1$ and $^2T_2$ states in the ultraviolet region, the latter state occurring at a shorter wavelength. By analogy, the CrO_4^{3-} bands at 350 and 270 mμ would be the $^2T_1$ and $^2T_2$ states respectively arising from a $t_1 \rightarrow 3t_2$ electron jump.

A band (not previously reported) around 410 to 430 mμ was observed in the alkaline earth fluorchromate apatites. As shown in Fig. 5 the band occurs as a shoulder on the 350-mμ band. Figure 5 (also Fig. 3) illustrates the broadness of the 700 to 750-mμ band which suggests that more than one transition is occurring in this region. Since the $t_1 \rightarrow e$ electron jump allows both a T_1 and T_2 state, it is possible that the 410 to 430 mμ band arises from the $^2T_2$ state while the $^2T_1$ state is one of the components of the broad band in the extreme red. The other component of the latter band would be the $^2T_2$ state originating from the $e \rightarrow t_2$ electron jump.

Table II summarizes the ultraviolet and visible absorption spectra of CrO_4^{3-} in apatite, the possible excited states and a comparison to the model proposed by Carrington and Symons (*6*) for the isoelectronic MnO_4^{2-} ion. As shown by Table II, the two oxyanions possess similar spectra. For both ions, the sum of the energies (reciprocal centimeters) of the $e \rightarrow t_2(^2T_2)$ and $t_1 \rightarrow e(^2T_2)$ transitions equals the energy of the $t_1 \rightarrow t_2(^2T_2)$ transition.

In conclusion, all of the apatites containing pentavalent chromium are green and have similar reflectance spectra. The positions at which the CrO_4^{3-} absorption bands occur are relatively independent of the composition (and lattice parameters) of the

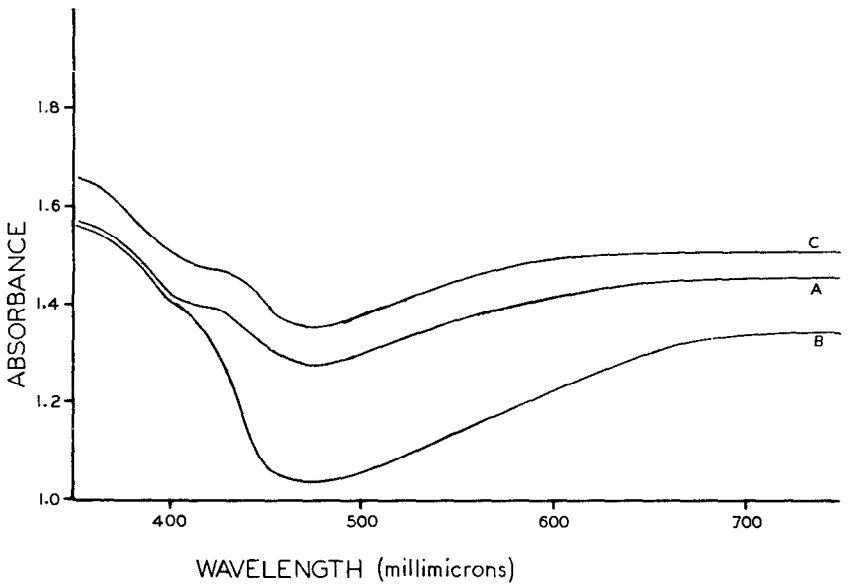

FIG. 5. Reflectance spectra of the alkaline-earth fluorchromate apatites.

$A = Ca_{10}(CrO_4)_6F_2$;
$B = Sr_{10}(CrO_4)_6F_2$;
$C = Ba_{10}(CrO_4)_6F_2$.

TABLE II

COMPARISON OF THE ULTRAVIOLET AND VISIBLE REFLECTANCE SPECTRUM OF CrO_4^{3-} IN APATITE TO THE MnO_4^{2-} SPECTRUM OF CARRINGTON AND SYMONS (6)

Electron Jump	Absorption Maxima for CrO_4^{3-} mμ	Reciprocal Centimeters	Excited State	Absorption Maxima for MnO_4^{2-} mμ	Reciprocal Centimeters
$t_1 \rightarrow t_2$	270	37,000	$^2T_2$	299	33,400
	350	28,600	$^2T_1$	351	28,490
$t_1 \rightarrow e$	~420	23,800	$^2T_2$	436	22,940
	~700	14,300	$^2T_1$	605	16,530
$e \rightarrow t_2$	~750	13,300	$^2T_2$	833	12,000

apatite. The origin of the absorption bands, though not proven, can be explained by the Ballhausen–Liehr molecular orbital model. Similar results for pentavalent manganese are discussed in the next section.

Manganese

Pentavalent manganese has a d^2 electronic configuration and a ground state designated by the Ballhausen–Liehr model as $(t_1)^6(2e)^2$. Considering the $t_1 \rightarrow e$, $e \rightarrow t_2$ and $t_1 \rightarrow t_2$ electron jumps, only the $^3A_2 \rightarrow {}^3T_1$ transitions are allowed. Since each of the above electron jumps gives rise to one $^3T_1$ state, the allowed spectrum of the MnO_4^{3-} ion consists of three bands.

Only two absorption bands have been observed for the MnO_4^{3-} ion in solution. These bands at 675 and 325 mμ have been assigned to the $t_1 \rightarrow e(^3T_1)$ and $t_1 \rightarrow t_2(^3T_1)$ transitions by Carrington and Symons (*6*) and Carrington and Schonland (*10*). By comparison, several absorption bands were reported by Kingsley et al. (*11*) for the MnO_4^{3-} ion in calcium chlorapatite and chlorspodiosite. The latter authors used the Ballhausen–Liehr model to interpret their spectra which contained weak nonallowed transitions.

In the present investigation, apatites containing only pentavalent manganese as the coloring ion were blue to turquoise at low-manganese concentrations. As will be shown, this color change was not primarily due to changes in the positions of the MnO_4^{3-} absorption bands.

The ultraviolet and visible absorption spectra of MnO_4^{3-} in barium chlorapatites, $Ba_{10}(PO_4)_{6-x}(MnO_4)_xCl_2$, are shown in Figs. 6 and 7, respectively. A strong band occurs in the vicinity of 315 mμ and a pair of weaker bands occur in the vicinity of 650 and 680 mμ. Assuming these are the three allowed

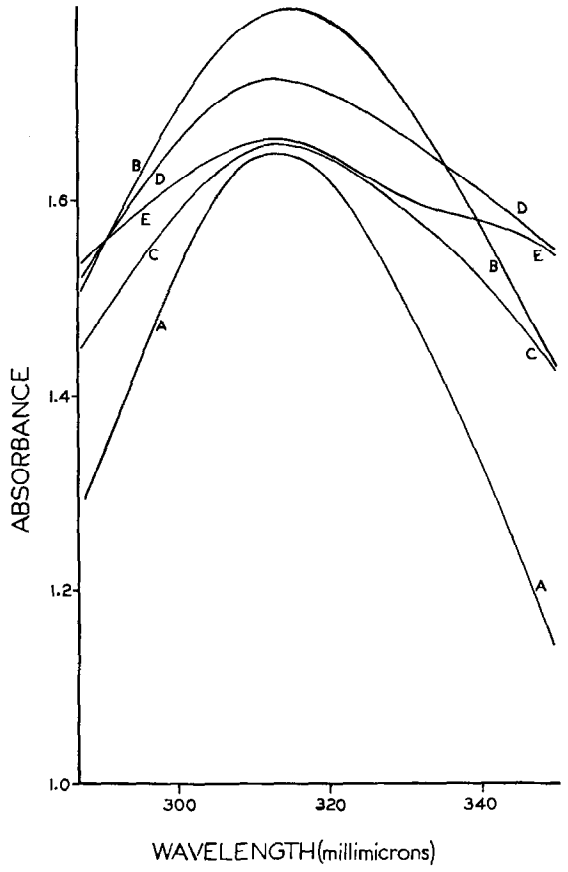

FIG. 6. Ultraviolet absorption band of the $Ba_{10}(PO_4)_{6-x}(MnO_4)_xCl_2$ apatites.

$A = Ba_{10}(PO_4)_{5.4}(MnO_4)_{0.6}Cl_2$;
$B = Ba_{10}(PO_4)_{4.8}(MnO_4)_{1.2}Cl_2$;
$C = Ba_{10}(PO_4)_{3.6}(MnO_4)_{2.4}Cl_2$;
$D = Ba_{10}(PO_4)_{1.2}(MnO_4)_{4.8}Cl_2$;
$E = Ba_{10}(MnO_4)_6Cl_2$.

transitions, the ultraviolet band must be due to the $t_1 \rightarrow t_2$ electron jump ($^3A_2 \rightarrow {}^3T_1$) while the visible bands are due to the $t_1 \rightarrow e$ and $e \rightarrow t_2$ electron jumps (also $^3A_2 \rightarrow {}^3T_1$). In agreement with Kingsley et al. (*11*) it is impossible to assign the bands at 650 or 680 mμ specifically to the $t_1 \rightarrow e$ or $e \rightarrow t_2$ transitions. The sum of the energies of the $t_1 \rightarrow e$ and $e \rightarrow t_2$ transitions predicts that the $t_1 \rightarrow t_2$ electron jump should occur around 330 mμ, which agrees well with the experimental value of 315 mμ. There is evidence of another transition occurring around 730 mμ in some of the spectra. This band is observed as a shoulder on the 680-mμ band and may be due to the $^1A_1$ state reported by Kingsley et al (*11*). Since this band was only occasionally observed, no further discussion is warranted.

Figure 7 shows that increases in the manganese concentration in barium chlorapatite increases the absorption due to the $t_1 \rightarrow e$ and $e \rightarrow t_2$ transitions. Although the substitution of manganese for phosphorus causes the apatite structure to expand, no shift is observed in the positions of the MnO_4^{3-} absorption bands. The ultraviolet absorption band in Fig. 6 shows no shift but the band broadens considerably. As a result of this broadening, increasing the concentration of manganese causes increasing absorption in the blue region of the spectrum and the body color of the apatite shifts towards the green. Hence, it is the broadening of the ultraviolet band which modifies the color of the barium chlorapatites containing manganese and not a change in the positions of the MnO_4^{3-} bands. As an example, Fig. 8 shows the transmission spectra of the $Ba_{10}(PO_4)_{6-x}(MnO_4)_xCl_2$ apatites.

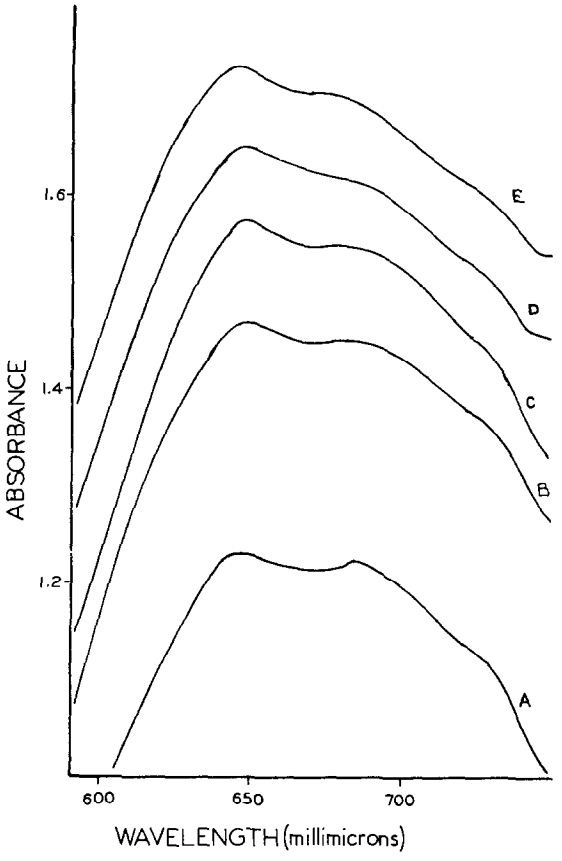

FIG. 7. Visible absorption bands of the $Ba_{10}(PO_4)_{6-x}(MnO_4)_xCl_2$ apatites.

$A = Ba_{10}(PO_4)_{5.4}(MnO_4)_{0.6}Cl_2$;
$B = Ba_{10}(PO_4)_{4.8}(MnO_4)_{1.2}Cl_2$;
$C = Ba_{10}(PO_4)_{3.6}(MnO_4)_{2.4}Cl_2$;
$D = Ba_{10}(PO_4)_{1.2}(MnO_4)_{4.8}Cl_2$;
$E = Ba_{10}(MnO_4)_6Cl_2$.

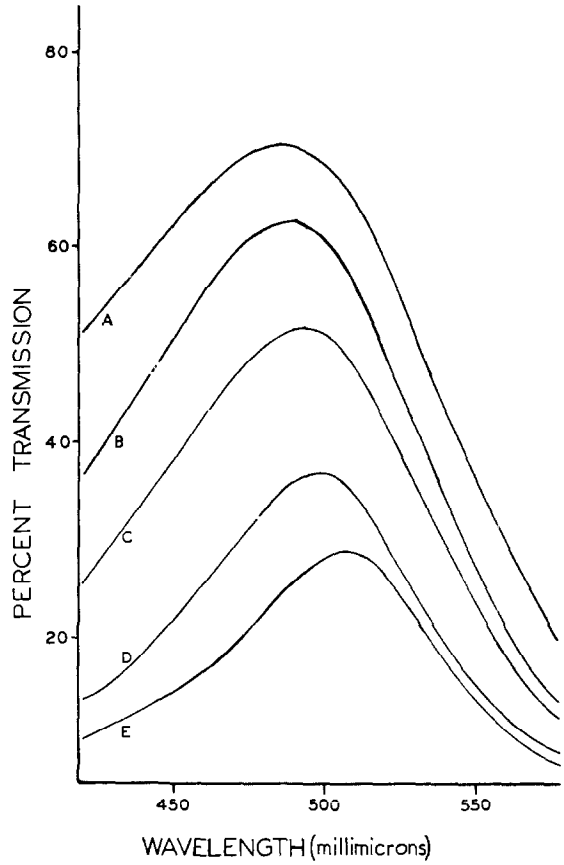

FIG. 8. Reflectance spectra of the $Ba_{10}(PO_4)_{6-x}(MnO_4)_xCl_2$ apatites.

$A = Ba_{10}(PO_4)_{5.4}(MnO_4)_{0.6}Cl_2$;
$B = Ba_{10}(PO_4)_{4.8}(MnO_4)_{1.2}Cl_2$;
$C = Ba_{10}(PO_4)_{3.6}(MnO_4)_{2.4}Cl_2$;
$D = Ba_{10}(PO_4)_{2.4}(MnO_4)_{3.6}Cl_2$;
$E = Ba_{10}(MnO_4)_6Cl_2$.

The above change in color with increasing MnO_4^{3-} content was also observed in the $Ba_{10}(PO_4)_{6-x}(MnO_4)_xF_2$, $Ba_{10}(VO_4)_{6-x}(MnO_4)_xF_2$ and $Ba_{10}(VO_4)_{6-x}(MnO_4)_xCl_2$ apatites. The reflectance spectra of the above series showed that the halide had no appreciable effect on the color and that for a given concentration of manganese, the vanadate apatites were greener than the phosphate apatites. The latter observation is attributed to the ultraviolet absorption of the VO_4^{3-} ion which also absorbs some of the blue wavelengths.

Figures 9 and 10 illustrate the ultraviolet and visible absorption bands respectively of various barium haloapatites containing manganese which differ in the composition of their pentavalent and/or halide ion contents. The similarity of these spectra indicates that the positions of the MnO_4^{3-} absorption bands in apatite are not appreciably affected by the composition of the tetrahedral and halide ion sites.

In contrast, substitutions in the divalent ion site affect the positions of the MnO_4^{3-} absorption bands. The complete substitution of strontium for barium produced a large lattice contraction and shifted the visible absorption bands of MnO_4^{3-} around 25 to 30 mμ to shorter wavelengths. The ultraviolet band shifted only 5 mμ in the same direction but it must be

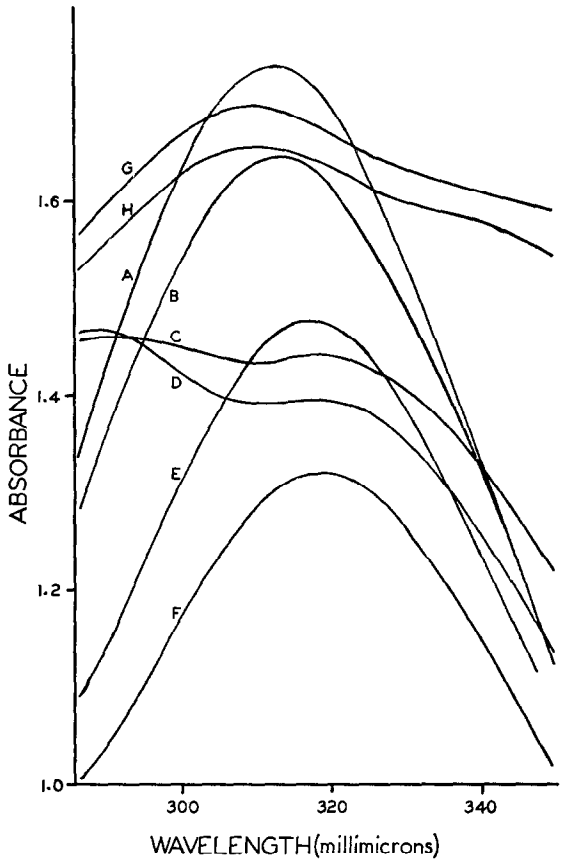

Fig. 9. Ultraviolet absorption band of barium haloapatites containing 10 mole % pentavalent manganese in the tetrahedral site.

$A = Ba_{10}(PO_4)_{5.4}(MnO_4)_{0.6}F_2$;
$B = Ba_{10}(PO_4)_{5.4}(MnO_4)_{0.6}Cl_2$;
$C = Ba_{10}(VO_4)_{5.4}(MnO_4)_{0.6}F_2$;
$D = Ba_{10}(VO_4)_{5.4}(MnO_4)_{0.6}Cl_2$;
$E = Ba_{10}(AsO_4)_{5.4}(MnO_4)_{0.6}F_2$;
$F = Ba_{10}(AsO_4)_{5.4}(MnO_4)_{0.6}Cl_2$;
$G = Ba_{10}(MnO_4)_6F_2$;
$H = Ba_{10}(MnO_4)_6Cl_2$.

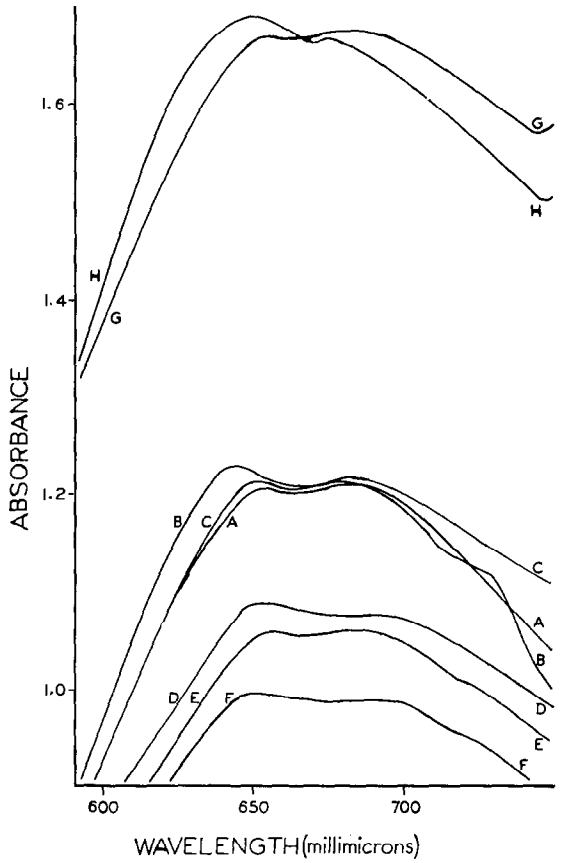

FIG. 10. Visible absorption bands of barium haloapatites containing 10 mole % pentavalent manganese in the tetrahedral site.

$A = Ba_{10}(PO_4)_{5.4}(MnO_4)_{0.6}F_2$;
$B = Ba_{10}(PO_4)_{5.4}(MnO_4)_{0.6}Cl_2$;
$C = Ba_{10}(VO_4)_{5.4}(MnO_4)_{0.6}F_2$;
$D = Ba_{10}(VO_4)_{5.4}(MnO_4)_{0.6}Cl_2$;
$E = Ba_{10}(AsO_4)_{5.4}(MnO_4)_{0.6}F_2$;
$F = Ba_{10}(AsO_4)_{5.4}(MnO_4)_{0.6}Cl_2$;
$G = Ba_{10}(MnO_4)_6F_2$;
$H = Ba_{10}(MnO_4)_6Cl_2$.

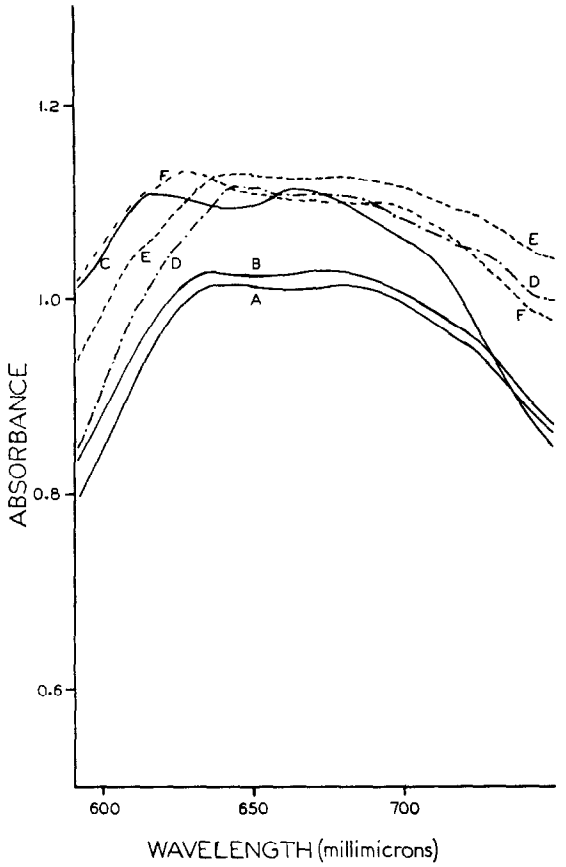

FIG. 11. Effect of strontium substituted for barium on the visible absorption bands of MnO_4^{3-} in apatite.

$A = SrBa_9(PO_4)_{5.4}(MnO_4)_{0.6}Cl_2$;
$B = Sr_2Ba_8(PO_4)_{5.4}(MnO_4)_{0.6}Cl_2$;
$C = Sr_{10}(PO_4)_{5.4}(MnO_4)_{0.6}Cl_2$;
$D = SrBa_9(VO_4)_{5.4}(MnO_4)_{0.6}Cl_2$;
$E = Sr_2Ba_8(VO_4)_{5.4}(MnO_4)_{0.6}Cl_2$;
$F = Sr_{10}(VO_4)_{5.4}(MnO_4)_{0.6}Cl_2$.

remembered that transition energies are measured in reciprocal centimeters. In all three bands the energy change is of the order of 600 reciprocal centimeters. Comparing the MnO_4^{3-} spectra in strontium and barium apatites (10-mole % manganese) of like compositions in their tetrahedral and halide sites, the 315, 650, and 680-mμ bands in the barium apatites shift to around 310, 625, and 650 mμ in the strontium apatites. An example of this shift in the visible absorption bands of the MnO_4^{3-} ion is illustrated in Fig. 11. As a result of the absorption band shifts, the strontium apatites are more of a true blue whereas the barium apatites are blue-turquoise.

In conclusion, barium apatites containing pentavalent manganese are blue to green and their reflectance spectra are characterized by absorption bands around 315, 650, and 680 mμ. The positions of the bands shift to shorter wavelengths when ions smaller than barium are substituted into the divalent ion site. The positions are not appreciably affected by substitutions into the tetrahedral and halide sites. The color can be shifted towards the green without changing the positions of the MnO_4^{3-} bands by substituting more manganese which broadens the ultraviolet absorption band to the extent that some blue is absorbed.

References

1. C. J. BALLHAUSEN AND A. D. LIEHR, Intensities in inorganic complexes. Part II. Tetrahedral Complexes, *J. Mol. Spectrosc.* **2**, 342–360 (1958).
2. A. CARRINGTON AND M. C. R. SYMONS, Structure and reactivity of the oxyanions of transition metals. Part I. The manganese oxyanions, *J. Chem. Soc. London* 3373–3380 (1956).
3. N. BAILEY AND M. C. R. SYMONS, Structure and reactivity of the oxyanions of transition metals. Part III. The hypochromate ion, *J. Chem. Soc. London* 203–207 (1956).
4. A. CARRINGTON, D. SCHONLAND, AND M. C. R. SYMONS, Structure and reactivity of the oxyanions of transition metals. Part IV. Some relations between electronic spectra and structure, *J. Chem. Soc. London* 659–665 (1957).
5. M. WOLFSBERG AND L. HELMHOLZ, The spectra and electronic structure of the tetrahedral ions MnO_4^-, CrO_4^{--} and ClO_4^-, *J. Chem. Phys.* **20**, 837–843 (1952).
6. A. CARRINGTON AND M. C. R. SYMONS (1960), "Structure and Reactivity of the Oxyanions of Transition Metals. Part IX. Electronic Spectra," *J. Chem. Soc. London*, Part I. 889–891.
7. A. CARRINGTON, D. J. E. INGRAM, K. A. K. LOTT, D. S. SCHONLAND, AND M. C. R. SYMONS, Electron resonance studies of transition metal oxyions. I. Experimental results for the manganate, hypomanganate, and ferrate ions, *Proc. Roy. Soc. Ser. A* **254**, 101–110 (1960).
8. C. DIKGRAAF, Similarities in the electronic spectra of $TiCl_4$ and $VOCl_3$, *Spectrochim. Acta* **21**, 1419–1421 (1965).
9. D. S. MCCLURE Electronic Spectra of Molecules and Ions in Crystals," 175 pp., Academic Press, Inc., New York, 1959.
10. A. CARRINGTON AND D. S. SCHONLAND, The absorption spectra of permanganate, manganate, and related oxyanions, *Mol. Phys.* **3**, 331–338 (1960).
11. J. D. KINGSLEY, J. S. PRENER, AND B. SEGALL, Spectroscopy of MnO_4^{3-} in calcium halophosphates, *Phys. Rev. A* **137**, 189–202 (1965).